Thermodynamics and Structure of Plate-Like Particle Dispersions

Delhorme, Maxime

2012

Thermodynamics and Structure of Plate-Like Particle Dispersions

Maxime Delhorme

Division of Theoretical Chemistry
Lund University, Sweden
and
ICB-UMR 6303 CNRS
Université de Bourgogne, Dijon, France

LUND UNIVERSITY

UNIVERSITÉ DE BOURGOGNE

Doctoral Thesis

The thesis will be publicly defended on Thursday 24th of May 2012, 10.30 in lecture hall B, Center for Chemistry and Chemical Engineering, Lund

The faculty opponents are Emanuela Del Gado,ETH Zurich, Switzerland and Roland Kjellander, University of Goteborg, Sweden

Front cover: Snapshot of a simulation representing a smectic B phase at a volume fraction of 3.6% and salt concentration of 1mM, see Paper II.

Doctoral Thesis

Theoretical Chemistry
Center for Chemistry and Chemical Engineering
Lund University
P.O. Box 124
SE-221 00 Lund
Sweden
and
Laboratoire Interdisciplinaire Carnot de Bourgogne,
UMR 6303 CNRS-Université de Bourgogne,
9 Av. A. Savary, BP 47870
F-21078 DIJON Cedex,
France

ISBN 978-91-7422-301-9
Printed by Media-Tryck, Lund University, Lund

DOKUMENTDATABLAD enl SIS 61 41 21

Organization LUND UNIVERSITY	Document name DOCTORAL DISSERTATION
	Date of issue April 18, 2012
	Sponsoring organization
Author(s) Maxime Delhorme	

Title and subtitle

Thermodynamics and Structure of Plate-Like Particle Dispersions

Abstract

A considerable amount of mineral particles are found to have a plate-like shape. The work in this thesis concerns theoretical investigations, using a Monte Carlo method, of the properties of such particles in aqueous solutions. The objectives were first to create a model that could capture the essential physics of clay suspensions and also to understand the role of thermodynamics in certain chemical processes. For all investigations, the results are related to experimental studies.

The acid-base behavior of clays have been studied, using the primitive model, and an excellent agreement between simulated and experimental results was found.

The formation of gel phases as a function of the charge anisotropy have also been investigated. Liquid-gel and sol-gel transitions are found to occur for high and moderate charge anisotropy, respectively. These transitions were also found to be size and salt dependent. In absence of charge anisotropy, a liquid-glass transition is reported.
The formation of smectic and columnar liquid crystals phases with plate-like particles has been found to be favored by a strong charge anisotropy, in opposition to what was observed for nematic phases. New liquid-crystal phases were also reported.

The stability and growth of nanoplatelets is discussed. It was found that the internal Coulombic repulsion could be the cause of the limited growth of C-S-H platelets. The influence of thermodynamics on the aggregation mode of such platelets was also investigated.

Key words: Statistical mechanics, Simulations, Plate-like particles, Liquid crystal phases, Model clay system, Gel phase, Glass phase, Charge anisotropy

Classification system and/or index termes (if any):

Supplementary bibliographical information:	Language English
ISSN and key title:	ISBN 978-91-7422-301-9

Recipient's notes	Number of pages 138	Price
	Security classification	

Signature Maxime Delhorme Date April 18, 2012

List of Papers

This thesis is based on the following papers, which will be referred to in the text by their Roman numerals. The papers are appended at the end of the thesis.

I **Paper I: Acid-Base Properties of 2:1 Clays. I. Modeling the Role of Electrostatics**
Maxime Delhorme, Christophe Labbez, Céline Caillet and Fabien Thomas
Langmuir, **26**, 9240-9249 (2010)

II **Paper II: Monte Carlo simulation of a Clay Inspired Model Suspension : The Role of Charge Anisotropy.**
Maxime Delhorme, Bo Jönsson and Christophe Labbez
submitted to *Soft Matter* (2012)

III **Paper III: Liquid Crystal Phases in Suspensions of Charged Plate-like Particles.**
Maxime Delhorme, Christophe Labbez and Bo Jönsson
accepted in *Phys. Chem. Lett.* (2012)

IV **Paper IV: Gel and Nematic Phases of Plate-like Particle Suspensions: Charge Anisotropy and Size Effects**
Maxime Delhorme, Bo Jönsson and Christophe Labbez
Manuscript (2012)

V **Paper V: The Growth and Stability of Nanoplatelets**
Maxime Delhorme, Christophe Labbez, André Nonat, Cliff Woodward and Bo Jönsson
Manuscript (2012)

List of Contributions

All papers employed own in-house computer codes/programs. These were developed together with the help and support from Bo Jönsson and Christophe Labbez.

I I conducted the MC simulations and took part in writing the article. MF calculation were conducted by C.L.

II I conducted all the simulations and participated in writing the article.

III I performed all the simulations and took part in writing the article.

IV I performed all calculations and had the main responsibility for writing the manuscript.

V All the MC simulations in 3D were conducted by me. Other simulations were done by B.J. I took part in the writing process of the manuscript.

Contents

Populärvetenskaplig sammanfattning på svenska

De flesta ser nog kemi som ett abstrakt och komplicerat ämne mestadels för att det behandlar byggstenar så små att de inte kan ses med blotta ögat. Men om man tänker på det så finns kemi överallt! Kemiska processer sker runtom och inuti oss oavbrutet: i våra kroppar där proteiners kemi spelar en stor roll, i produkter som schampo och tandkräm, i cement som används för att bygga våra hus etc. Det borde därför inte komma som någon stor överraskning att enormt mycket resurser läggs på att förstå olika kemiska processer.

Så vad är då dessa osynliga beståndsdelar som kemi handlar om? Jag tror mig våga påstå att alla någon gång hört talas om atomer och molekyler (varav de senare utgörs av en grupp sammanlänkade atomer). Atomer och molekyler är inte alltid neutrala, d.v.s., dom kan bära en elektrisk laddning. Övergången från en neutral till en elektriskt laddad enhet kan exempelvis ske när atomer eller molekyler kommer i kontakt med ett lösningsmedel, vilket är fallet när ett salt löses upp i vatten och blir till fria joner. Fler exempel på molekyler som blir laddade i vatten är proteiner, virus, polyelektrolyter etc. Liksom magneters positiva och negativa poler attraherar varandra, kommer den erhållna elektriska laddningen i molekyler spela en viktig roll för hur dessa interagerar. Bland många andra faktorer såsom tex partikelgeometrin, spelar laddningen en primär roll i kemiska processer. Fysikalisk kemi fokuserar på att förstå de processer som äger rum när så kallade kolloidala partiklar interagerar i en lösning under olika förhållanden. Att utföra experiment med partiklar i storleksordningen 1-1000 nanometer är inte trivialt. Här kommer beräkningskemin in som en kraftfullt komplement. Genom att använda matematiska och fysikaliska modeller, så eftersträvar man att simulera de experimentellt erhållna resultaten och samtidigt förstå de underliggande mekanismerna och drivkrafterna på en nivå som ej är möjlig på något annat sätt.

Den här avhandlingen behandlar Monte Carlo-simuleringar av diskformade mineralpartiklar. I första projektet undersöktes hur antalet laddningar på en

diskformad mineralpartikel varierar som funktion av pH i en saltlösning av olika koncentrationer. Därefter studerades hur denna laddningsfördelning påverkar bildandet av geler och flytande kristallina faser. Genom denna studie upptäcktes nya termodynamiskt stabila faser vilket kan leda till utvecklandet av nya material. Slutligen så studerades tillväxten av diskformade nanopartiklar och deras interaktioner under förhållande jämförbara med de förekommande i en cementblandning.

Popular science summary in English

Most people see chemistry as an abstract and complicated subject because it deals with species that can not be seen with bare eyes. But if one think about it, chemistry is everywhere! Chemical processes happen all around you and inside you everyday : there is chemistry in the human body where proteins play a great role, in shampoo bottles, the toothpaste, in the cement that is used to build houses. Then it should not come as a surprise that so much effort are put into understanding chemical processes.

So what are those invisible species that chemistry is dealing with ? I can say with few doubts that everyone have heard about atoms and molecules (the latter being an assembly of atoms). Atoms and molecules are not always neutral species, i.e, they can carry an electrical charge (in this case atoms turn into ions). This transition from a neutral to a charged species can occur when the species are put into a solvent (like water). This is the case for example with salt that dissolves in water and form ions. Examples of molecules that becomes charged in an solvent are numerous : proteins, virus, polyeletrolytes ... But why is this electrical charge so important ? Like for magnets, where a positive pole will attract a negative one, the species will start to interact according to their charge. Among other factors like the shape of the particles, the role played by the charges in chemical processes is fundamental.
Physical chemistry focuses on the understanding of the behavior of such small particles (called colloïdal particles) in solution. Nevertheless, down to this scale, the experimental study of colloïdal dispersions is not trivial. In this context computational chemistry happens to be very useful. By the use of mathematical and physical models, one tries to simulate the results obtained by experiments and this way one can access properties that are not obtainable by other means. Hence, it is a complementary technique to experiments.

This thesis deals with simulations, using Metropolis Monte Carlo method, of mineral particles. In a first project I investigate how the number of charges on mineral particles varies when emerged into a salt solution. In a second

project the influence of the charge carried by the particles in the formation of the gels and liquid-crystals is studied. One of the striking result is the discovery of new liquid crystal phases which could lead to the development of new materials. Finally I studied the growth of nanoplatelets and their interaction in conditions comparable to the one encountered in cement paste.

Résumé simplifié en français

Beaucoup de personnes voient la chimie comme un sujet abstrait et difficile parce qu'elle concerne l'étude d'éléments invisibles à l'oeil nu. Mais, en y réfléchissant, la chimie est partout! Des processus chimiques se déroulent tout autour de nous et aussi en nous tous les jours : dans le corps humain oú les protéines jouent un grand rôle, dans les bouteilles de shampoing, dans le dentifrice, dans le ciment utilisé pour bâtir les maisons... Cela ne devrait donc être une surprise pour personne qu'autant d'efforts soient employés dans l'étude des processus chimiques.

Qu'elles sont ces epèces invisibles avec lesquelles la chimie fonctionne ? Je pense pouvoir affirmer avec peu de doutes que vous avez tous entendu parlé des atomes et des molécules (qui sont un assemblage d'atomes). Atomes et molécules ne sont pas toujours des espèces neutres, c'est-à-dire, elles peuvent porter une charge électrique (dans ce cas, les atomes sont appelés des ions). Cette transformation d'une espèce chargé à une espèce neutre peut se dérouler lorsque la particule est plongée dans un solvant (comme l'eau). C'est le cas par exemple lorsque l'on met du sel dans l'eau et que des ions sont formés. Les exemples de particules qui deviennent chargées dans un solvant sont nombreux: protéines, virus, polyélectrolytes ... Mais pourquoi cette charge électrique est elle si importante ? Comme pour les aimants, où le pôle positif attire le négatif, les espèces vont commencer à interagir selon leur charge. Parmi d'autres facteurs, tel que la forme de la particule, le rôle joué par les charges dans les processus chimiques est primordial.
La physico-chimie se concentre sur la compréhension du comportement de telles petites particules (appelés particules colloïdales) lorsqu'elles sont immergées dans une solution. Néanmoins, à cette échelle, l'étude expérimentale des dispersions colloïdales n'est pas triviale. Dans ce contexte, les simulations informatiques se trouvent être très utile. Elles ont pour but, par l'emploi de modèles physiques et mathématiques, d'essayer de reproduire les résultats obtenus expérimentalement et d'accéder à des valeurs qu'aucunes autres techniques ne peuvent procurer. Elles sont donc complémentaires aux expériences.

Cette thèse traite de simulations moléculaires, réalisées à l'aide de l'algorithme de Metropolis, de particules minérales en forme de disques. Dans un premier projet, l'évolution du nombre de charges sur une particule en fonction de la concentration en sel est étudiée. Dans un second temps, l'influence de la charge portée par les particules sur la formation des phases de gels et de cristaux liquides est examinée. Un des résultats les plus marquant est la découverte de nouvelles phases de cristaux liquides qui pourraient permettre le développement de nouveaux matériaux. Enfin, la croissance de nano particules et leurs interactions sont étudiées dans des conditions similaires à celles rencontrées dans les pâtes de ciment.

Chapter 1

Introduction

Nano-particles with a plate-like geometry are common in nature and synthetic materials, or at least can well be approximated as such. The most common examples are minerals like clays, gibbsite and calcium silicate hydrate (C-S-H) the main hydrate found in hydrated cement paste. Plate-like particles are also found in organic chemistry, where bonding molecules into a discotic macromolecule is possible. Clays and C-S-H dispersions in aqueous solutions is the main focus of this work. Their geometry combined, in some cases, with a charge heterogeneity, e.g. clays, give rise to complex and nonisotropic inter-particle potentials. The sign and the magnitude of the overall interparticle potential depends strongly on the anisotropy, concentration, and charge heterogeneity of the particles as well as on pH of the aqueous solution, salt nature and concentration. This results in a vast zoo of atypical macroscopic states and behaviors when dispersed in aqueous solution. As an example, clays are known to form gels at low particle volume fractions (ϕ) and liquid crystals when concentrated. Many industrial applications take advantage of these properties e.g. drilling, plastics [1], construction materials, papers, softeners, photonics and photovoltaic cells. However, the understanding of those systems is still in its infancy.

Clays and C-S-H particles belong to the domain of colloids as at least one of their dimensions is in the nanometer range. Since the forties, the stability of colloidal dispersions in aqueous solution has been rationalized with the help of the DLVO theory [2,3], that combines a short range attractive (van der Waals) potential with a long range electrostatic repulsion. Indeed, a strong attraction

[1] S. Laschat, A. Baro, N. Steinke, F. Giesselmann, C. Hägele, G. Scalia, R. Judele, E. Kapatsina, S. Sauer, A. Schreivogel, and M. Tosoni, Angew. Chem. Int. Ed. **46**, 4832 (2007).

[2] B. V. Derjaguin and L. Landau, Acta Phys. Chim. URSS **14**, 633 (1941).

[3] E. J. W. Verwey and J. T. G. Overbeek, *Theory of the Stability of Lyophobic Colloids* (Elsevier Publishing Company Inc., Amsterdam, 1948).

can force particles to coagulate and lead to a phase separation, whereas a dispersion under strong repulsion can remain stabilized for years [4]. Unfortunately, the DLVO theory is valid only for a limited range of conditions. In particular, it is valid in the thermodynamic limit of infinite particle dilution and for weakly coupled systems, i.e. where ion-ion correlations are not predominant. What is more, the DLVO theory focus on the simplest case: dispersions of charged isotropic particles. The lack of a generalized DLVO like effective potential, on one hand, and of extensive computer simulations on dispersion of anisotropic particles, on the other hand, best explains our poor understanding of these complex systems and the motivations of this work.

Here, computer simulations are used to identify, at the microscopic scale, the different chemical and physical processes when plate-like particles are immersed into a salt solution in an attempt to rationalize macroscopic observables. In Paper I a detailed investigation of the charging process of the titrable edges of natural clay particles is performed in comparison with potentiometric titration experiments. In papers II - IV, the modeling of dispersions of plate-like particles in 1-1 salt solutions in various conditions is considered. Paper II deals with the formation of gels in the low ϕ range and discusses in some details the similarities and differences of the model results with experimental observations on laponite and montmorillonite. Paper III prospects the high ϕ range where several liquid crystal phases are found. In Paper IV a detailed investigation of the geometry and charge anisotropy effects on the formation of gel and nematic phases is performed and discussed in light of recent experimental findings on dispersions of various mineral plate-like particles. Finally, paper V describes the growth and interaction between homogeneously charged disc particles in presence of multivalent counterions in relation to observations on C-S-H nano-hydrates.

The book is organized as follow. First the theoretical background and simulation techniques are described and then in section VII conclusions on this work are drawn. For those who do not want to dwell on a full length article, a brief summary of the important results is also presented. The papers are presented in the appendix at the end of the book.

[4] D. F. Evans and H. Wennerström, *The Colloid Domain where Physics, Chemistry, Technology and Biology meet* (VCH Publishers Inc., New York, 1994).

Chapter 2

System

An interesting point when one works with physical chemistry is the necessity to connect the different scales. As a matter of fact, the connection between a macroscopic system in a gel state (as obtained in an experiment) with the organization of particles and the interparticle forces at a nanometer scale (as obtained by computer simulation) is not trivial. One thing I would like to point out in this book is the route one has to follow to be able to work this way up through the different scales and to link a real experimental system constituted of billions of particles moving around a solution to the hundreds of platelets that are included in a computer simulation.

2.1 Structure

This thesis deals with the simulation of plate-like particles and the results are compared, when possible, to experimental systems of mineral disk-like particles from diverse origin (clays[5], gibbsite [6], cement [7]...). Montmorillonite and laponite clays and C-S-H particles (found in cement paste) are classified as phyllosilicates. It means that their crystalline structure is constituted of an octahedral layer sandwiched by two tetrahedral layers of silicate. In the case of clays, the layers are made of covalently bonded silicate atoms that organize in tetrahedral or octahedral sites. The tetrahedral sites share three of their apex while the last one is linked to the octahedral site. Exchangeable metal ions are present in both type of sites, and can be substituted by ions

[5] G. W. Brindley and J. J. Comer, *THE STRUCTURE AND MORPHOLOGY OF A KAOLIN CLAY FROM LES EYZIES (FRANCE).*

[6] H. Saalfeld and M. Wedde, Zeitschrift fur Kristallographie **139**, 129 (1974).

[7] J. J. Chen, J. J. Thomas, H. F. W. Taylor, and H. M. Jennings, Cement and Concrete Research **34**, 1499 (2004).

of lower valency. This produces a negative structural charge. The cleavage of the crystalline structure gives rise to titratable sites on the edges, which sign and magnitude depend on pH, electrolyte nature and concentration. Natural clays e.g. montmorillonite have a thickness of 1 nm but a diameter that can vary between 100 and 1000 nm. Laponite, a synthetic clay, has a smaller diameter than montmorillonite, typically 20-50 nm, for the same thickness. The crystalline structure of gibbsite contains stacks of sheets formed by aluminum hydroxide octahedral sites. The aluminum ions can be exchanged with anions of lower valency introducing this way a structural charge. Titratable sites are also present on the rims as a consequence of the cleavage of the crystalline structure. Gibbsite particles are often of a hexagonal shape of thickness 10-15 nm and diameter between 100-400 nm. The C-S-H particles are formed through the conjugated reactions of dissolution of tricalcium silicate grains (C_3S) and of precipitation. These particles are in the form of nanoplatelets with dimensions 60 x 30 x 5 nm^3. The C-S-H particles carry titratable silanol sites both on the edges and on the basal surface. At high pH and in presence of calcium salt solutions they are found to be highly negatively charged [8].

2.2 Gels

A gel is a non-ergodic disordered state that displays no long-ranged order. Macroscopically, it is reached when the solution do not flow any longer. The gel phase originates from attractive interactions between particles and thus are formed by percolated particles that form an infinite elastic network. The characteristic length of the network between two adjacent junctions, is much larger than the size of the particle. Moreover, if E is the depth of the attractive potential between two junctions: $E/k_BT \gg 1$ [9]. Experimentally gel phases can be characterized by the static structure factor S(q) obtained from scattering experiments. As a matter of fact, the S(q) curve presents two peaks, the first at large q reflects the short interparticle distance between aggregated particles and the second at low q, followed by a power law tail, reflects the characteristic size and fractal nature of the growing network. Gel and glass present different dynamic properties due to their different characteristic lengths. This can be investigated with the help of dynamic light scattering (DLS) [10,11]. Note that, from simulations, the static structure factor, and dynamic properties (through

[8] C. Labbez, B. Jönsson, I. Pochard, A. Nonat, and B. Cabane, J. Phys. Chem. B **110**, 9219 (2006).

[9] H. Tanaka, J. Meunier, and D. Bonn, Phys. Rev. E **69**, 031404 (2004).

[10] S. Jabbari-Farouji, G. Wegdam, and D. Bonn, Phys. Rev. Lett. **99**, 021402 (2007).

[11] S. Jabbari-Farouji, H. Tanaka, G. Wegdam, and D. Bonn, Phys. Rev. E **78**, 061405 (2008).

time autocorrelation functions) are also reachable [12].

2.3 Attractive glass

Glasses are non-ergodic disordered states but unlike the gel, their elasticity originates from caging effects. The formation of an attractive glass is then possible when attractive interactions are at play in the colloidal system. Typically such a phase would form if the volume fraction ϕ is high enough and if the depth of the attractive well E is of the order of k_BT [9]. Nevertheless, even if attractive interactions are active, the repulsive interactions still play the main role, contrarily to the gel phase. As experimental evidence of the formation of a glass phase, the static structure factor presents only one peak at a distance characteristic of the interparticle distance and shows only a small change when the system ages. According to Jabbari-Farouji et al. [11], attractive glass displays features of both glass and gel when experimentally characterized. Their detection in computer simulations is not trivial.

2.4 Wigner glass

A glass phase can also be found at very low volume fraction and in the absence of attractive interactions. In this case the caging effect originates from the double layer repulsion between the particles. Thus, the particles do not form a network and are spatially disconnected. The formation of the repulsive glass is favored by low ionic strengths as the double layer repulsion is known to decrease when increasing salt. All experimental evidences discussed in the previous section stay true for a Wigner glass. But, unlike the gel phase, a Wigner glass should melt when a dilution is performed on it. Recently Ruzicka et al[13] and Jabbari-Farouji et al [11] reported the formation of a Wigner glass for high volume fractions for a system of laponite platelets. This controversial result is discussed in paper II.

2.5 Liquid crystals

Due to their geometry, plate-like particles have the ability to form liquid crystals at high volume fractions. In these phases, particles present a long-ranged positional and/or orientational order but the phase preserves the properties

[12] E. DelGado and W. Kob, Soft Matter **6**, 1547 (2010).

[13] B. Ruzicka, L. Zulian, E. Zaccarelli, M. Sztucki, A. Moussaid, and G. Ruocco, Phys. Rev. Lett. **104**, 085701 (2010).

of liquids. Onsager rationalized the formation of liquid crystal phases for uncharged platelets [14,15] and explained, counter-intuitively, that their formation had an entropic origin. Indeed the origin of these phase comes from the competition between the orientational entropy, that tends to favor isotropic phase, with the translational entropy that favors liquid crystals. The main classes of liquid crystals encountered with plate-like particles are the nematic phase, the smectic phase and the columnar phase, presented in figure 2.1.

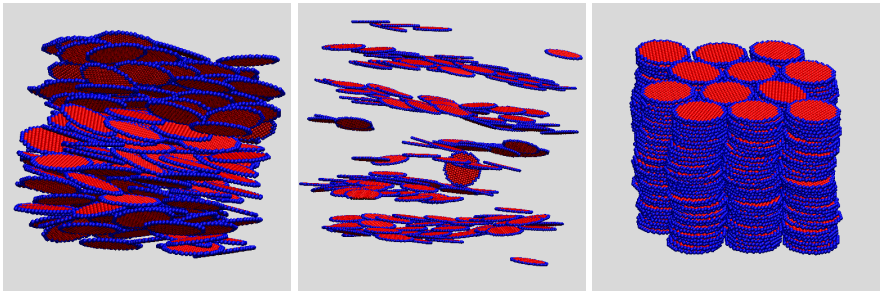

Figure 2.1: Representation of the liquid crystal phases encountered with platelets. a) Nematic phase, b) Smectic phase and c) Columnar phase.

While all of these phases present an orientational order they differ by the positional correlation between the platelets. The nematic phase present no positional order whereas the smectic phase, that is constituted of platelets gathered in parallel sheets, has a one dimensional positional order. Finally, the columnar phase, where the particles are organized in stacks including a large number of platelets, have a two-dimensional positional order. While the formation of such phases with uncharged platelets is now well understood [16], the influence on the liquid crystal formation of charged platelets remains unclear. This is investigated in papers II - IV.

2.6 Coarse graining

Ideally one would try to describe a system as accurately as possible. Unfortunately, as described above, a mineral platelet has a minimum diameter of ~ 50 nm which represents about 30000 atoms. With todays processors, computer simulations can only be done with a limited number of species (around 10^5 species for Monte Carlo as an example). It becomes then mandatory to find

[14] L. Onsager, Phys. Rev. **62**, 558 (1942).
[15] L. Onsager, Ann. N.Y. Acad. Sci. **51**, 627 (1949).
[16] J. A. C. Veerman and D. Frenkel, Phys. Rev. A **45**, 5632 (1992).

a way to reduce the number of species in the simulations. The first way is to consider smaller particles than the actual studied system. This is actually not a big issue if one is interested in a qualitative description of the physical phenomenon that happens in a system. A second way would be to vulgarize the description of some species. That is where coarse graining comes into play. It consists of gathering several units of any constituent of the system into a single grain. The coarse graining has to be done with some care. While decreasing the level of description of the model or the degrees of freedom of the particles, one has to make sure to preserve the principal physical properties. For instance, the detailed description of a charge distribution can be lost when merging several point charges into a single one. In all papers, several different coarse grain models have been used : in paper I, the detailed description of the structure is replaced by hard grains to account for the finite size of the particle. In papers II - IV, the description of the particles evolves with the separation between themselves and in the last article, one platelet is represented as a collection of charged grains. This method has been shown to reduce the computing time up to several orders of magnitude and will be further discussed in chapter 6.1.

Chapter 3

Statistical Mechanics and Thermodynamics

At a microscopic scale, a solution can be seen as an infernal mixture of species in constant motion. How can one link this chaotic states to a macroscopic thermodynamic property as obtained from experiments (pressure, temperature, ...) ? Statistical thermodynamics is the Rosetta stone that provides the connection between the two scales. Originally from the 19th century, statistical thermodynamics is based on two postulates. The postulate about equal a priori probability states that [17] "an isolated system in equilibrium is equally likely to be in any of its accessible microscopic quantum states", and links macroscopic properties of an isolated system to probability theories. Indeed, many of the macroscopic properties are time-averaged properties, which makes them difficult to access. Instead, the ergodic hypothesis allows to access this properties by considering ensemble average. It states : " the time average of any mechanical variable is equal to the ensemble average of the same variable". An ensemble here is defined as an important number of replica of the system.

3.1 Statistical mechanical ensembles

It is common to start looking into statistical thermodynamics [18,19] considering an isolated system with constant energy U, volume V, and number of

[17] R. Kjellander, *The basis of statistical thermodynamics or My favorite path to thermodynamics and beyond* (University of Göteborg, Göteborg, Sweden, 1991).

[18] T. L. Hill, *An Introduction to Statistical Thermododynamics* (Dover Publications Inc., New York, 1986).

[19] D. A. McQuarrie, *Statistical Mechanics* (Harper Collins, New York, 1976).

particles N. In this ensemble, defined as the microcanonical ensemble, the entropy S is given by :

$$S = k_{\mathrm{B}} \ln \Omega_{U,V,N} \tag{3.1}$$

where k_{B} is the Boltzmann constant, and $\Omega_{U,V,N}$ is the microcanonical partition function. It refers to the number of accessible quantum states of the system. In an isolated system this function is sufficient to determine a large amount of thermodynamic properties (P, T, μ, ...). Partition functions are accessible from other ensemble. In the canonical ensemble, where the number of particles N, the volume V and the temperature T are kept constant, it is defined from the microcanonical partition function as :

$$Q_{N,V,T} = \sum_{U} \Omega_{U,V,N} \; e^{-\beta U} \tag{3.2}$$

where β = $1/k_B$T. $Q_{N,V,T}$ is referred as the canonical partition function. Finally, in the grand canonical ensemble, where exchange in particles between the system and a reservoir is allowed, the grand potential, takes the form :

$$\Xi_{\mu,V,T} = \sum_{N} Q_{N,V,T} \; e^{\beta \mu N} \tag{3.3}$$

where μ is the chemical potential of a particle in the system. As for the microcanonical ensemble, thermodynamic properties are derivable from these two last ensemble. This way, the Helmholtz' free energy is defined in the canonical ensemble as :

$$A_{N,V,T} = -k_{\mathrm{B}} T \ln Q_{N,V,T} \tag{3.4}$$

While the product of the pressure and the volume can be related to the grand potential:

$$PV = k_{\mathrm{B}} T \ln \Xi_{\mu,V,T} \tag{3.5}$$

3.2 Classical statistical mechanics

When considering a continuum approach rather than a quantum mechanical one, one has to integrate over all the classical "states" of a system. The canonical partition function becomes :

$$Q_{N,V,T} = \frac{1}{N! h^{3N}} \iint e^{-\beta H(p^N, q^N)} dp^N dq^N \tag{3.6}$$

where h is the Planck's constant, $H(p^N, q^N)$ the Hamiltonian of an N components system of coordinates q and momenta p. As the particles are indistinguishable the factor $N!$ comes into play in the denominator. The Hamiltonian

of the system is indeed the total energy of the system and can be written as the sum of kinetic energy $K(p^N)$ and a potential energy $U(q^N)$, which gives :

$$H(p^N, q^N) = U(q^N) + K(p^N) \tag{3.7}$$

Then, if one integrates over the kinetic part, equation (3.6) can be simplified as follow :

$$Q_{N,V,T} = \frac{1}{N!\Lambda^{3N}} \int e^{-\beta U(q^N)} dq^N \tag{3.8}$$

where $\Lambda = h/\sqrt{2\pi m k_B T}$ and m is the mass of one particle.

3.3 Protonation state

As stated in chapter 2, the studied minerals carry titrable groups, clays on the edges and C-S-H on all surfaces. Several types of groups exist and are formed by a metal atom (Me) linked to a hydroxyl group. The total charge carried by those groups may vary and can be entire or fractional. A typical protonation/deprotonation reaction can be written as:

$$-Me - OH \longleftrightarrow -Me - O^- + H^+ \tag{3.9}$$

The intrinsic dissociation constant of above reaction is defined by :

$$K_{Me-O} = \frac{a_{H^+} a_{Me-O}}{a_{Me-OH}} = \frac{\gamma_{H^+}\gamma_{Me-O}}{\gamma_{Me-OH}} \cdot \frac{c_{H^+} c_{Me-O}}{c_{Me-OH}} \tag{3.10}$$

where a_i are the activities, c_i the concentrations and γ_i activity coefficients of the species i. One can then express the pKa in terms:

$$pKa = -log\frac{\gamma_{H^+}\gamma_{Me-O}}{\gamma_{Me-OH}} - log\frac{c_{H^+} c_{Me-O}}{c_{Me-OH}} \tag{3.11}$$

Let's denote $\Gamma = \gamma_{H^+}\gamma_{Me-O}/\gamma_{Me-OH}$ and pH the negative logarithm of the proton concentration, we obtain:

$$pKa = -log\Gamma - log\frac{c_{Me-O}}{c_{Me-OH}} + pH \Longleftrightarrow -log\frac{c_{Me-O}}{c_{Me-OH}} = -log\Gamma - (pH - pKa) \tag{3.12}$$

where $\frac{c_{Me-O}}{c_{Me-OH}}$ is the probability of deprotonation of the group, and can be written as a free energy difference:

$$\beta\Delta A_{MeOH \to MeO} = -ln\frac{c_{Me-O}}{c_{Me-OH}} = -ln\Gamma - ln10 \cdot (pH - pKa) \tag{3.13}$$

$-ln\Gamma$ is defined as the sum of excess chemical potentials of all the species. This can be used [20,21] to derive an MC move as explain in section 5.3.4 .

[20] M. Ullner, B. Jönsson, and P.-O. Widmark, J. Chem. Phys. **100**, 3365 (1994).
[21] M. Lund and B. Jönsson, Biochemistry **44**, 5722 (2005).

Chapter 4

Intermolecular Interactions

The most accurate way to calculate the total interaction between two particles would be to solve the Hamiltonian of this system. This quantum mechanical calculation is at least very expensive and at worst impossible to carry out. It is then necessary to use interactions like electrostatic interactions, exchange repulsion or van der Waals interactions [22] to describe the behavior between particles [23]. The aim of this chapter is not to give a full descriptions of all the existing interactions but rather to give a brief description of those used in papers I - V.

4.1 Coulombic interactions

Two charged species i and j sitting at a fixed distance r_{ij} from one another will experience the field emitted by the other molecule. This strong and long-ranged interaction is known as the Coulombic interaction [24] and reads :

$$u(r_{ij}) = \frac{q_i q_j}{4\pi\epsilon_0 r_{ij}} \tag{4.1}$$

where q are the charges of the species and ϵ_0 is the permittivity of vacuum (ϵ_0 = $8.854.10^{12}$ $C^2 J^{-1} m^{-1}$). This description of the interplay between two charged species does not take into account any influence of a surrounding medium and remains only correct in vacuum. When the charged molecules are immersed into a solvent, the solvent molecule rearrange according to the total emitted field. The effect is particularly important in a highly polar solvent like water. It can be derived that for purely dipolar solvent the electro-

[22] V. A. Parsegian, *van der Waals Forces* (Cambridge University Press, New York, 2006).
[23] J. Israelachvili, *Intermolecular and Surface Forces* (Academic Press, London, 1991), 2nd edn.
[24] J. D. Jackson, *Classical Electrodynamis* (John Wiley & Sons, Inc., New York, 1999).

static interactions scale with a factor of ϵ_r^{-1}, where ϵ_r is the dielectric constant, changing the Coulomb interaction to its solvent average form :

$$w(r_{ij}) = \frac{q_i q_j}{4\pi\epsilon_0\epsilon_r r_{ij}} \tag{4.2}$$

The most commonly used solvent is water and its dielectric constant is equal to 80 at room temperature. Indeed, dielectric constant is known to be temperature dependent as well as salt concentration dependent [25,26]. The averaged Coulomb interaction is then a free energy. When salt is introduced in the solution, it will influence the interactions the same way the solvent does. It becomes possible to derive the expression of the Coulomb interaction when a simple 1:1 salt is taken into account. This is known as the Debye-Hückel potential [4] , derived from the linearized Debye-Hückel theory [27] :

$$u(r_{ij}) = \frac{q_i q_j}{4\pi\epsilon_0\epsilon_r}\frac{e^{-\kappa r_{ij}}}{r_{ij}} \tag{4.3}$$

where κ is the inverse Debye screening length and is defined as :

$$\kappa^2 = \frac{\sum_i (z_i e)^2 c_i}{\epsilon_0\epsilon_r k_B T} \tag{4.4}$$

where c_i and z_i are the concentration and the valency of the ionic species i, respectively. Scaling the Coulomb interaction with $e^{-\kappa r_{ij}}$ simply represents the decay of the electrostatic interactions due to the salt screening.
Note that in all papers included in the thesis, ϵ_r is considered constant throughout space. This approximation is often used in simulation of colloïds and is known to give a good agreement between simulations and experiments for several types of processes [28], like the charging process for instance.

4.2 Short ranged interactions

Due to Pauli's exclusion principle, it is known that two particles repel one an other at short separation. The simplest way to account for the finite size of the particles in a simulation is to consider them as impenetrable hard spheres. This is denoted as the hard sphere model :

$$u(r_{ij}) = \begin{cases} 0 & r_{ij} > \sigma_{ij} \\ +\infty & r_{ij} < \sigma_{ij} \end{cases} \tag{4.5}$$

[25] J. Hubbard and L. Onsager, J. Chem. Phys. **67**, 4850 (1977).
[26] J. M. Cailol, D. Levesque, and J. J. Weis, J. Chem. Phys. **85**, 6645 (1986).
[27] P. Debye and E. Huckel, Z. Physik **24**, 185 (1923).
[28] M. Lund, B. Jönsson, and C. E. Woodward, J. Chem. Phys. **126**, 225103 (2007).

where σ_{ij} is the minimum separation between species i and j, $\sigma_{ij} = (d_i + d_j)/2$, and d is the diameter. This potential presents inconvenience in the fact that it is not a continuous function and causes problems when one want to derive properties at contact, see e.g. force calculation in chapter 6.3. One way to circumvent this problem is to use a soft repulsive interaction. One of them is the 6-12 Lennard-Jones (LJ) potential expressed by :

$$u(r) = 4\epsilon((\frac{\sigma_{ij}}{r_{ij}})^{12} - (\frac{\sigma_{ij}}{r_{ij}})^{6}) \tag{4.6}$$

where ϵ describes the strength of the interaction. This potential combines the short range attractive part in r^{-6} from the van der Waals attraction with a soft repulsion that decays as r^{-12}. In fact, it is one of the most widely used potentials in the literature. One way to get rid of the attractive part and to preserve soft repulsion is to shift and truncate this potential. This gives rise to the shifted and truncated LJ potential :

$$u(r_{ij}) = \begin{cases} 4\epsilon((\frac{\sigma_{ij}}{r_{ij}})^{12} - (\frac{\sigma_{ij}}{r_{ij}})^{6}) + \epsilon & r_{ij} < \sqrt[6]{2}\sigma_{ij} \\ 0 & r_{ij} > \sqrt[6]{2}\sigma_{ij} \end{cases} \tag{4.7}$$

It has the advantage of being less long-ranged than a pure r^{-12} soft repulsive potential.
Note that the combination of the Coulombic interaction and the hard sphere model is called the primitive model [18] and is often used in simulations of colloïdal systems.

4.2.1 Effective pair potentials

The use of *effective* pair potentials is an attractive and efficient way to model / simulate complex systems [29] like the ones of interest in this work. Indeed, in such systems a brute force calculation that would involve, in addition to the many atoms constituting the particles, a molecular description of the *dense* solvent, i.e. water concentration is roughly 55 mol/l, and all the ions is extremely challenging if not stupid. The philosophy behind the term *effective*, instead, consists in *averaging* over all the configurations of some of the components. An effective pair potential has by its very nature, the characteristics of a free energy. As an example, equation 4.2, introduced in preceding section, is an effective pair Coulombs potential where the solvent molecules has been averaged out and reduced to one single quantity that is the dielectric constant ϵ_r. Similarly, equation 4.3 for the screened Coulombs interaction is a

[29] M. Turesson, B. Jönsson, and C. Labbez, Langmuir **28**, 4926 (2012).

effective potential between two point charges where the degrees of freedom of the solvent molecules and ions have been averaged over.

On a more general ground, the effective pair potential, or the potential of mean force between two macro-particles ($w^{(2)}(R)$), defines the average work needed to bring particles i and j from infinite separation to R,

$$w^{(2)}(R) = -\int_{\infty}^{R} F_{ij}(r)\mathrm{d}r \tag{4.8}$$

where $F_{ij}(r)$ is the average force acting on the macro-particles i and j when separated a distance r. $w^{(2)}(R)$ is also related to the probability P(R) of finding two macro-particles a distance r,

$$P(R) \propto exp(-w^{(2)}(R)/k_B T) \tag{4.9}$$

Chapter 5

Monte Carlo Simulations

Many different simulation techniques from diverse origin exist. Many of them are based on statistical mechanics, like Molecular Dynamic (MD), Brownian Dynamic (BD) or Monte Carlo (MC) [30,31,32]. The one of interest here is the MC simulation technique. While MD and BD are dynamic simulations and calculated properties are time-averaged properties, MC is a stochastic technique and works with ensemble average. From MC, it is possible to evaluate definite multidimensional integrals, like eq. 3.8, which are intractable with analytic techniques. It also provides several advantages inherent to this technique: i) the equilibrium is quickly reached, ii) it allows the use of a large number of ensembles and iii) it allows unphysical displacements of the particles.

5.1 Thermal averages and importance sampling

Actually, MC simulations can not be used to evaluate directly integrals of the form $\int e^{-\beta U(q^N)} dq^N$ but indeed they make reachable thermal average of any observable ξ which expression is given by:

$$< \xi >= \frac{\int \xi(q^N) e^{-\beta U(q^N)} dq^N}{\int e^{-\beta U(q^N)} dq^N} \tag{5.1}$$

Technically, this can be done by averaging over a high number of reproduc-

[30] D. Frenkel and B. Smit, *Understanding Molecular Simulation* (Academic Press, San Diego, 1996).

[31] M. P. Allen and D. J. Tildesley, *Computer Simulation of Liquids* (Oxford University Press, Oxford, 1989).

[32] Landau and Binder, *A Guide to Monte Carlo Simulations in Statistical Physics* (Cambridge University Press, Cambridge, 2000).

tions of the system which are representative of an ensemble. Those are generated stochastically with the help of random numbers. Obviously, the more configurations of the system are generated and averaged over, the more accurate the evaluation of the observable. Note that, it is important to use a good random number generator if one wants to avoid bias in the sampling. This will not be developed in this book, for more detailed information see reference [32]. However, at this point, one problem emerges. Most of the generated configurations of the system will not give any informations about the observable of interest. Then an important number of reproductions would be needed to evaluate correctly $< \xi >$ and it would turn MC simulations into a slow and useless technique. Indeed only configurations which gives informations of interest should be sampled. This problem is solved with the method of the Metropolis Importance Sampling [33]. The idea is to sample configurations with a probability proportional to their Boltzmann weight :

$$P(q_i^N) = \frac{e^{-\beta U_i(q_i^N)}}{\int e^{-\beta U(q_i^N)} dq_i^N} \tag{5.2}$$

where i, refers to the i:th configuration of the system. Then it follows that the probability of going from the configuration i to j is defined as :

$$\frac{P(q_i^N)}{P(q_j^N)} = e^{-\beta(U(q_i^N) - U(q_j^N))} \tag{5.3}$$

Equation 5.3 is actually very useful as it defines the Metropolis acceptance test in a MC simulation in the canonical ensemble, that is : the probability of acceptance to go from configuration i to j is :

$$\alpha_{acc}(i \to j) = min(1, e^{-\beta(U(q_i^N) - U(q_j^N))}) \tag{5.4}$$

The use of this criteria will be detailed in the next section.

5.2 The procedure

In this section, the procedure for a typical MC simulation is described. The first step is to choose a box of any form (cubic, cylindrical, ...), where the model particles are placed (randomly or not). Unfortunately the number of sites (including particles, or other species) that a MC simulation can handle is relatively limited, i.e about 10^6. Hopefully the thermodynamic limit is reached for really small systems, and few particles are needed to get a proper

[33] N. A. Metropolis, A. W. Rosenbluth, M. N. Rosenbluth, A. Teller, and E. Teller, J. Chem. Phys. **21**, 1087 (1953).

statistical average. At this point a problem that may arise, depending on the type simulation box used, is that the surface of the box will have a strong influence on the particles. Or, when interested in bulk properties, one wants to avoid this effect. One way to circumvent it, is to apply periodic boundary conditions to the box. It consists of reproducing the main simulation box in all directions. This creates an artificial periodicity that mimics the bulk conditions. The next step is to run the Markov chain that consists of several operations :

- Choose a particle at random in the simulation box.
- Apply a random move to the particle. Different kind of moves are developed in the next section.
- Calculate the energy difference (using the chosen potential(s)) between the new and the old configuration. $\Delta U = U_{new} - U_{old}$.
- Apply the Metropolis acceptance criteria. For that, one needs to generate a random number, denoted $Rand \in [0, 1]$. The move is accepted if $Rand < \alpha_{acc}$ (Eq. 5.4), else rejected.
- If the move is accepted, sample the desired properties.
- Start again from first step.

Usually a first run is done without any sampling. This is called the equilibration run. The aim of this operation is to make sure that the system has reached equilibrium before one starts sampling equilibrium properties. It is actually in the second run, called the production run, that all properties are sampled. On the paper, running MC simulations seems like an easy task. But sometimes it is a bit more intricate. Highly concentrated systems or systems in (semi-)crystalline phases might reveal themselves tricky to equilibrate due to their slow "natural" dynamics. As an example figure 5.1 shows the evolution of the total energy of a system constituted of 200 platelike particles build of 199 sites at a high volume fraction of 21 % and at a salt concentration of 1 mM. The system needs between 2 and 2.5 10^6 cycles (= moves per particles) to be equilibrated, which corresponds to 8 days of calculation time on 8 processors. This is a typical behavior when one deals with simulations of liquid crystal phases (papers II - IV). At higher volume fraction up to 4 months were necessary to equilibrate the systems.
A way to help the simulations to converge faster is to implement in the Markov chain the use of cluster moves, see after 5.3.2.

5.3 Monte Carlo moves

When a particle is moved in the simulation box, the detailed balance criteria has to be fulfilled, i.e. in equilibrium the probability of accepting a move from

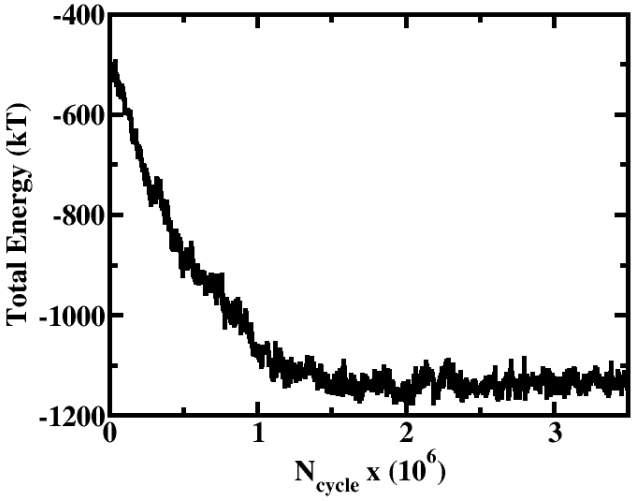

Figure 5.1: Evolution of the total energy as a function of the number of cycles for a system of 200 platelets constituted of 199 sites for a volume fraction of 21 % and a salt concentration of 1mM.

configuration 1 to 2 has to be the same as the reverse move (from 2 to 1). This implies :

$$P(1)\pi(1 \to 2) = P(2)\pi(2 \to 1) \tag{5.5}$$

where *P(x)* is the probability to be in state x and $\pi(a \to b)$ is the transition probability to go from configuration *a to b*. Eq. 5.5 can be rewritten :

$$\frac{\pi(1 \to 2)}{\pi(2 \to 1)} = \frac{P(2)}{P(1)} = e^{-\beta(U(2)-U(1))} \tag{5.6}$$

5.3.1 Single particle displacements

Single particle displacements are the simplest move that exists in a MC simulation. They consist in choosing one particle at random and translate or rotate it a certain distance or angle. The amplitude of the moves are usually set as input parameters of the MC runs. As a rule of thumbs, displacement parameters are usually set so that the acceptance ratio is between 20 and 40%.

5.3.2 Cluster moves

Sometimes moving the particles and sampling the configurational space might be difficult. A trick to help the sampling is to create a "bias" in the MC simulation by using unphysical moves that are more likely to be accepted. A cluster move [30,34]consists in gathering several particles into a cluster and to make a collective displacement (translation or rotation) of all particles that belong to the cluster. The acceptance criteria of such a move is :

$$\alpha_{acc}^{cluster} = min(1, e^{-\beta\Delta U} \prod_{kl} \frac{1 - p^{new}(k,l)}{1 - p^{old}(k,l)}) \tag{5.7}$$

where p(k,l) is the probability for particle k (inside the cluster) and l (outside the cluster) to be in the cluster. This simply means that the number of total particles in the cluster should be the same before and after the move. The criteria of affiliation of one particle to the cluster remains of the choice of the user as the results do not depend on the cluster form. This is actually satisfactory since it allows to adapt the cluster shape according to the structure and geometry of the studied system. In papers II -IV, instead of using the common spherical cluster, where all particles included in a sphere of radius R from a random particle belong to the cluster, infinite thin slit and sphero-cylindrical clusters have been developed. A 2D sketch of the cluster moves with a sphero-cylinder is drawn in figure 5.2.

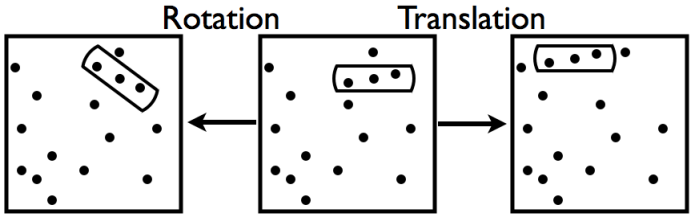

Figure 5.2: Schematic representation of a cluster move. The cluster described is the sphero-cylindrical cluster and the figure on the left hand side describes the result of a rotation while on the right hand side, the result of a translation.

The infinite slit cluster has a fixed thickness (defined in the input parameters).

[34] H. L. Gordon and J. P. Valleau, Mol. Simul. **14**, 361 (1995).

It allows the common displacement of aligned particles. This has been shown to be efficient when dealing with layered liquid crystal phases, e.g. Smectic B and columnar phases. The sphero-cylinder cluster has also a fixed thickness but a variable radius taken at random and allows the displacement of close proximity particles like aggregated particles. It has been shown to be efficient for gel phases. Rotation moves of the slit cluster is, however, limited to small angles, typically $\sim 5 - 6^{\circ}$, since artefacts in the cluster configuration can occur due to the periodic boundary conditions, as illustrated in figure 5.3.

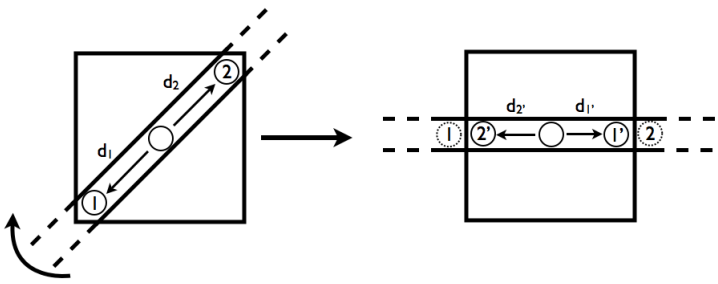

Figure 5.3: Schematic representation of the rejection of a rotation move of an infinite cluster. In this case the periodic boundary conditions lead to the creation of an artefact in the cluster.

In this particular example, particles 1 and 2 are moved out of the simulation box after rotation of the cluster. Once the periodic boundary conditions applied, the particles are found in the new positions 1' and 2' with the new interparticle distances inside the cluster different from the original ones, i.e. $d_1 \neq d_{1'}$ and $d_2 \neq d_{2'}$. In this case the detailed balance is not respected and the MC move is rejected.

5.3.3 Addition or deletion of species

When simulating in the grand canonical ensemble, the simulation box is connected to a reservoir of particles of appropriate species (salt, macroions ...). This implies that besides of the normal moves, the species have to be allowed to enter and leave the simulation box. This is done by trying random additions or deletions of the species in the box [35]. The acceptance criteria for insertion is defined as :

[35] J. P. Valleau and K. Cohen, J. Chem. Phys. **72**, 5935 (1980).

$$\alpha_{acc}^{insertion} = min(1, \frac{V}{\Lambda^3(N+1)} e^{(\beta(\mu-\Delta U))}) \tag{5.8}$$

and for deletion as:

$$\alpha_{acc}^{deletion} = min(1, \frac{N\Lambda^3}{V} e^{(-\beta(\mu+\Delta U))}) \tag{5.9}$$

where ΔU is the energy difference between the new configuration where the species are added or removed and the old configuration, V is the volume of the box, and N the number of species. When changing the number of charged species, one has to be careful to keep electroneutrality in the box. This is done by adding a number of molecules whose total charge is zero.

5.3.4 Grand canonical titration method

From the thermodynamic derivation in section 3.3 we extracted the free energy difference upon deprotonation of a titrable site. This can been used to develop a MC titration move at the level of the primitive model where the protons are treated implicitly and for which the energy difference can be written as:

$$\Delta U = \Delta U^{el} \pm kT \ln 10(\mathrm{pH} - \mathrm{p}K_0) \tag{5.10}$$

where ΔU^{el} is the electrostatic part and the second term on the right hand side accounts for the chemical effects through the log decimal of the intrinsic dissociation constant ($\mathrm{p}K_0$) evaluated in the appropriate thermodynamic reference state (ideality). Note that the minus sign is for deprotonation and the plus sign for protonation.
In practice, the method consists in (i) changing the charge status of the site taken at random and (ii) moving an arbitrary salt ion in or out from the simulation box to maintain the electroneutrality of the system. Steps (ii) makes eq. 5.10 incorrect by an energetic term associated with the move of the simple salt ion. A grand canonical titration method has been proposed [36] to remedy this problem. It relies on the idea that the titration can be decomposed in several steps. As an example the (de)protonation can be decomposed in two successive steps that involve i) the (de)protonation of the surface and ii) the exchange of the ion couple (H^+, B^-) with the bulk. For deprotonation, the acceptance rule thus reads:

$$\alpha^{deprotonation} = min(1, \frac{N_B}{V} e^{-\beta\mu_B} e^{-\beta\Delta U^{el}} e^{+\ln 10(\mathrm{pH}-\mathrm{p}K_0)}) \tag{5.11}$$

[36] C. Labbez and B. Jönsson, Lect. Notes Comp. Sci. **66**, 4699 (2007).

and for protonation :

$$\alpha^{protonation} = min(1, \frac{V}{N_B + 1} e^{+\beta\mu_B} e^{-\beta\Delta U^{el}} e^{-\ln 10(\mathrm{pH}-\mathrm{p}K_0)}) \tag{5.12}$$

where μ_{B^-} is the chemical potential of the simple salt anion B^-.
This method was used in paper I.

Chapter 6

Simulations Techniques

An important number of simulation programs (open source and commercial codes) are available, e.g. Gromacs [37](MD), Faunus [38] (MC), Molcas [39] (QM). These codes can, in principle, be handled by a large community of expert and non-expert users. All the codes used during my PhD are in-house written. It is relevant to mention here that a lot of effort were devoted into code development and optimization to obtain the results presented in this work. The purpose of this section is to highlight some of the techniques I used to improve the efficiency of Monte Carlo simulations and to analyze the results.

6.1 Distance dependent coarse graining

As stated in chapter 2, one of the most efficient way to decrease the computing time is to coarse grain the system. For this purpose, a distance dependent coarse graining was developed and used in the simulations presented in papers II-IV. Its principle relies on the idea that at large inter-particle separation the use of the same level of particle description as at short separation is not necessary when calculating the inter-particle interactions. Indeed, a detailed description at short separation and a punctual net charge at large separation give almost the same degree of accuracy. Figure 6.1 illustrates the particle description employed on the fly during simulations as a function of their separation for calculating the interactions.
In practice, three levels of description were used, as described in Fig. 6.1, delimited by two cut-off distances, f_1 and f_2. These conveniently allow to

[37] http://www.gromacs.org/.
[38] http://faunus.sourceforge.net.
[39] http://www.molcas.org/.

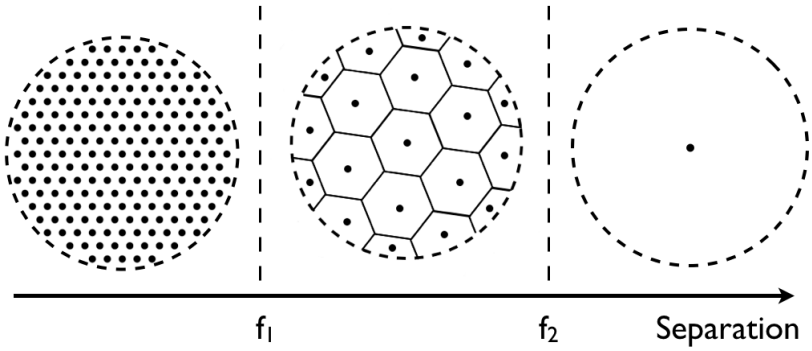

Figure 6.1: Description of a particle as a function of its separation with respect to the others when calculating the interactions. At short separations, the full description is used; at intermediate separations, the sites are gathered into a collection of hexagonal patches and at large separations the particle is reduced to a punctual net charge. f_1 and f_2 are user defined cut-off distances, see the text for more details.

switch from one level of description to another during a simulation. f_1 and f_2 were determined by comparing the energy of interaction between two rings of appropriate charge and size with those obtained with the level of description described above for a large range of screening length. At a given κ, the cut-off distance was defined as the distance that gives an energy difference of $\sim 10^{-6}$ kT. The obtained points were interpolated with a simple exponential function as exemplified in Figure 6.2. Note that the procedure has to be repeated for all particle sizes and net charges considered.

6.2 Phase characterization

6.2.1 Nematic order parameter

A convenient way to characterize a nematic phase in a simulation is to calculate the nematic order parameter (S) which is a measurable quantity in an experiment. S is bound between zero and unity and measures the long range orientational order characteristic of a nematic phase. It takes the value of unity in a sample where all the platelets are perfectly orthogonal to the sample director, $\mathbf{n}$, defined as the spatial and ensemble average of the particle normal vectors, $\mathbf{u}$. $S = 0$ when they are randomly oriented. As a matter of fact, $S^2 = P_2(r \to \infty)$ where $P_2(r)$ is the second Legendre polynomial of the azimuthal angle between the normal vectors of two platelets. $P_2 = 1$ when the normals are parallel and $P_2 = -1/2$ when perpendicular. Typically, $S \sim 0.4$

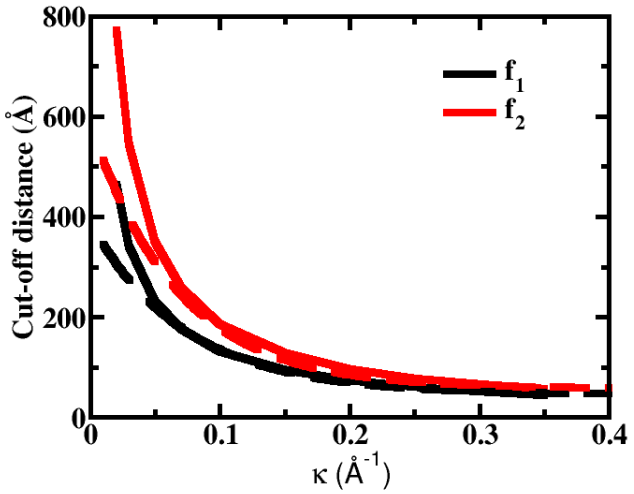

Figure 6.2: Cut-off distances, f_1 and f_2, as a function of the inverse screening length κ for particles having a diameter of 150 Å, a net charge of -103 e and patches with a net charge of -19e. The dashed lines show the result of the exponential fits.

at the isotropic/nematic phase transition. In addition, S is found to increase rapidly with ϕ at the isotropic/nematic phase transition which allows to define quite accurately its position, as exemplified in figure 6.3.
Although S can in principle be calculated from P_2 extrapolated at large r it is in most of the cases computationally cumbersome since this presupposes that simulations are run on large systems. More conveniently, S may be obtained from the evaluation of the director [40]. Indeed, S can be written as the following ensemble average,

$$S = \frac{1}{2N}\langle\sum_{i}^{N} 3\mathbf{u}_i \cdot \mathbf{n} - 1\rangle \tag{6.1}$$

where N is the total number of particles. The length scale of director fluctuations is large compared to a typical simulation box size, and, consequently, a single director apply to the simulated sample at any instant. That is, the typical length scale of a liquid crystal without defect is considerably larger

[40] M. Allen, G. T. Evans, and D. Frenkel, *Hard Convex body fluids* (John Wiley & Sons, Inc., New York, 1993).

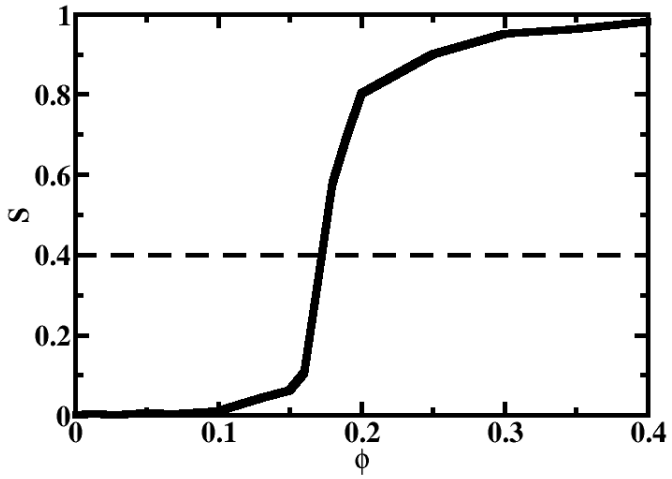

Figure 6.3: Nematic order parameter as a function of ϕ calculated for a system of 200 uncharged platelets constituted of 199 sites and of diameter 150 Å. S is found to increase rapidly at the isotropic/nematic transition.

than what is so far possible to simulate. During the course of a simulation the director, however, slowly fluctuates, i.e. change direction. The difficulty to determine the nematic order parameter is, thus, to determine the director. For this purpose two routes were followed. The first consists in calculating the director for each configuration, since $\mathbf{u}_i = -\mathbf{u}_i$ (no polarity), $\mathbf{n}$ can be calculated like $\mathbf{n} = \sum \pm \mathbf{u}_i$, and S from equation 6.1. The second is based on the maximization of S with respect to rotation of $\mathbf{n}$. It can be shown [40] that writing $S = \mathbf{n} \cdot \mathbf{Q} \cdot \mathbf{n}$, where $\mathbf{Q}$ is the order parameter tensor, reduces the problem to diagonalizing $\mathbf{Q} \cdot \mathbf{Q}$, and may be written as,

$$< Q >= \frac{1}{N} \langle \sum_{i=1}^{N} \frac{3}{2} \mathbf{u}_i \cdot \mathbf{u}_i - \frac{1}{2} \mathbf{I} \rangle \tag{6.2}$$

where $\mathbf{I}$ is the identity matrix. The eigenvalues of this tensor are λ_+, λ_0 and λ_- in order of decreasing size. They are directly related to the order nematic parameter as :

$$\begin{cases} \lambda_+ = S \\ \lambda_0 = -S/2 \\ \lambda_- = -S/2 \end{cases} \tag{6.3}$$

The eigenvector corresponding to λ_+ gives the director.

Figure 6.4 shows the behavior of the calculated nematic order parameter as a function of the number of MC cycles at two different volume fractions using the two methods described above. At low particle concentrations, i.e in the isotropic phase (Fig. 6.4 left), S values obtained from equation 6.3 are converged after $\sim$ 500 cycles. From the direct evaluation of the director, equation 6.1, the results converge more slowly. Equation 6.3 is more accurate at low volume fraction but both techniques are equivalent at high volume fraction, see Fig. 6.4 right). In this example, S obtained from λ_+ and equation 6.1 are indistinguishable and after a few cycles, converge to $\sim$ 0.9. From this comparison and further tests, not presented here, it was found that S determined from λ_+ was the more stable one. All the calculations of S presented in the papers were thus determined from λ_+.

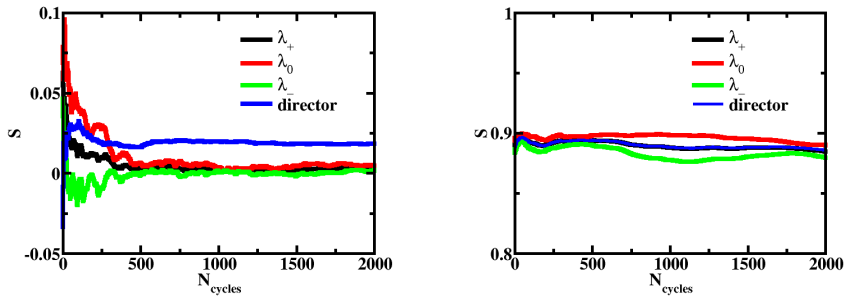

Figure 6.4: Nematic order parameter obtained from equations 6.3 and 6.1, see the text for more details. Simulations are performed for a system of 200 platelets constituted of 199 sites, of diameter 150 Å and net charge Z_{net}=-151e. The salt concentration is 10 mM and the particle volume fractions are chosen such as ϕ=7% (left), and 18% (right).

6.2.2 Columnar phases

In paper III formations of columnar phases are described. In addition to the usual radial distributions, several characteristic structural parameters were determined to characterize them. These are the average inter-columnar distance, the average intra-columnar distance and the average angle of the particles with the columnar phase director as depicted in Figure 6.5
To do so, the following procedure is used and repeated for all particles of a considered configuration. A "columnar" cylinder (dotted) and "planar" sphero-cylinder (dashed lines) centered on a chosen particle are created ori-

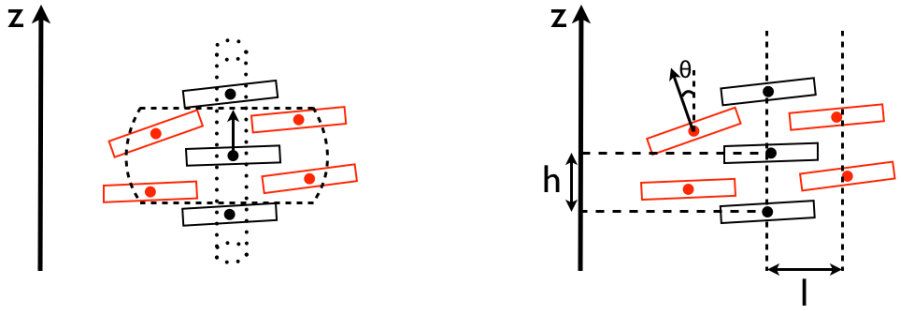

Figure 6.5: Schematic representation of the columnar structural parameters; h: intra-columnar distance; l: inter-columnar distance, θ average particle angle.

ented according to its normal vector. The columnar cylinder is used to determine the nearest neighbors in the same column called *intra-columnar* (black particles). The planar sphero cylinder (dashed line) is used to find the neighbors in the adjacent columns belonging to the same or nearest planes designated as *inter-columnar* (red particles). The geometrical parameters are then recorded as a function of the number of nearest intra- and inter-columnar neighbors. The analysis is included in the Markov chain and takes place typically every 4000 cycles. At the end of the MC simulations the distribution of the different structural parameters are determined. Note that the dimensions of the two geometrical probes have to be adapted according to the columnar phase studied.

6.2.3 Gels

As explained in chapter 5, MC simulations do not provide access to dynamic quantities. Then to capture the gel formation from the simulations, two parameters are considered: the percolation and the elasticity of the system. The percolation is studied through the connectivity of the particles in the simulation box. Two platelets are considered to be "connected" neighbors if the separation between a site in one platelet is within 15Å of a site in the other. Several connected platelets are said to form a cluster. From these definitions several quantities are calculated like:

- The average number of neighbors for a platelet in a cluster ($\langle N_{nei} \rangle$).
- The average number of platelets in a cluster ($\langle N_{cl} \rangle$).
- The probability to find a particle in a cluster of size X ($\langle P_X^{cl} \rangle$).

- The average fraction of particles in a cluster = $\int_2^N P_X^{cl} dX$ ($\langle f^{cl} \rangle$).

The elasticity of the suspension is evaluated calculating the average squared force acting on a particle. For that, the squared force is calculated for the three Cartesian components: $\langle F_x^2 \rangle$, $\langle F_y^2 \rangle$ and $\langle F_z^2 \rangle$ where:

$$\langle F_x^2 \rangle = - \left\langle \left(\frac{\partial w(R)}{\partial x} \right)^2 \right\rangle \tag{6.4}$$

The total average squared force is then considered to be the arithmetic average of the three Cartesian components.

6.3 Potential of mean force between two platelets

In paper V the potential of mean force, pmf, between two charged platelets is studied at the level of the primitive model. The pmf is calculated within a closed cylindrical cell where the particles are allowed to move along the axis of revolution of the cell z.
The pmf calculation of two platelets quickly becomes computer demanding as their size grow. This is related to the difficulty to move the platelets due to their geometrical anisotropy, the number of species involved and the magnitude of the interactions in play. For this reason the calculation of the pmf from the platelet radial distribution function, c.f. equation 4.9, turns out to be rather inefficient although cluster moves were employed and the sampling was split into several windows. Alternatively, the pmf can be extracted from the inter-particle force calculated at fixed positions R. The force can either be calculated at contact with the colloids or at the cylinder mid-plane, see below. The latter was found to be the more efficient mainly because the ion density at the mid-plane is much lower than at contact with the colloids.
Figure 6.6 compares the calculated pmf between two platelets with 19 sites (50 Å in diameter) immersed in a 10 mM 2:1 salt solution at $\phi = 0.013$ using the different approaches described above. In paper V the two last techniques have been used to sample the free energy since they are either easier to use or more accurate.

In the following we will assume two colloids decorated with n_s charged sites, immersed in a salt solution containing N_i ions. In addition, the sites and ions are considered as charged Lennard-Jones (LJ) particles.

6.3.1 Contact force approach

The mean force between two platelets for a fixed colloid center-to-center separation R can be evaluated at contact [30,31]. It can be written as the sum of four distinct terms, see eq. 6.5. The two first terms are the direct Coulombs and LJ

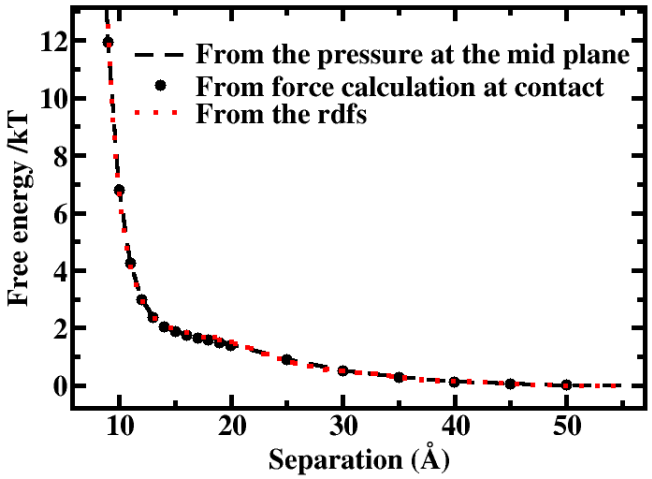

Figure 6.6: Potential of mean force between two platelets with 19 sites (50 Å in diameter) immersed in a 10 mM 2:1 salt solution at $\phi = 0.013$ obtained from three different approaches. Full curve: mid-plane approach; symbols: contact force approach; dotted curve: radial distribution function approach.

forces between the colloids. The two last terms are the ensemble average of the electrostatic and LJ forces exerted on the colloids by the surrounding ions.

$$F(R) = - \left\langle \sum_{i=1}^{n_s} \sum_{j=1}^{n_s} \left(\frac{\partial u^{el}(r_{s_i s_j})}{\partial R} + \frac{\partial u^{LJ}(r_{s_i s_j})}{\partial R} \right) \right\rangle - \left\langle \sum_{i=1}^{N_i} \sum_{j=1}^{n_s} \left(\frac{\partial u^{el}(r_{i s_j})}{\partial R} + \frac{\partial u^{LJ}(r_{i s_j})}{\partial R} \right) \right\rangle \tag{6.5}$$

6.3.2 Mid-plane approach

The mean force can also be evaluated over the mid-plane [41,42] ($z = 0$) for a fixed colloid center-to-center separation R along the main axis, z, of the cylinder cell. By doing so, the total mean force can be divided into three

[41] P. Linse, Adv. Polym. Sci. **185**, 111 (2005).
[42] J. Z. Wu, D. Bratko, H. W. Blanch, and J. Prausnitz, J. Chem. Phys. **111**, 7084 (1999).

terms according to 6.6.

$$F(R) = F^{el}(R) + F^{LJ}(R) + F^{id}(R) \tag{6.6}$$

The terms $F^{el}(R)$ and $F^{LJ}(R)$, are calculated by summing all Coulomb and LJ forces between species residing on different sides of the mid-plane. The last term is the ideal contribution, which can conveniently be defined as

$$\beta F^{id}(R) = [\rho_I(z = 0) - \rho_I(z = \pm L/2)]A \tag{6.7}$$

where $\rho_I(z = 0)$ and $\rho_I(z = \pm L/2)$ are the ion densities at the mid-plane and at the cylinder end walls of cross-sectional area A.

Chapter 7

Summary of Results and Concluding Remarks

7.1 Charging process of 2:1 clays

The role of electrostatic interactions on the acid-base titration of various natural clays is investigated in paper I. With a model that is shown to include the main physics, we demonstrate that the observed pH shift in the titration curves with the ionic strength originates from electrostatic interactions between the titratable edge charges and the permanent basal charge [43,44,45]. An excellent agreement is found between simulations and experimental titrating results. When looking at the titration of clay platelets stacks, like e.g. Illite, the point of zero net proton charge (PZNPC) is found to decrease when increasing the number of sheets in the stacks. These results are used to rationalize the order of apparent PZNPC (or PZSE in the case of pyrophyllite) found in the literature: Pyrophyllite ($4 <$ PZSE < 4.5) $<$ Illite $<$ Montmorillonite. Finally the mean field approach is shown to fail to describe the acid-base behavior of clays for low pH and high salt concentration.

7.2 Gel and glass formations

When attractive interactions are at play in a clay suspension, gels form at low volume fractions. They arise from the strong attraction between positively charged edges and negatively charged basal planes. Their formation is shown

[43] B. Baeyens and M. Bradbury, J. Contam. Hydrol **27**, 199 (1997).
[44] M. Duc, F. Gaboriaud, and F. Thomas, J. Colloid Interface Sci. **289**, 148 (2005).
[45] E. Tombácz and M. Szekeres, Appl. Clay Sci. **27**, 75 (2004).

to be enhanced for large particle sizes, high charge anisotropy and low salt concentration. A detailed study of the gel structure indicates that they are formed by a network of platelets organized in a mixture of "House of Cards" and "Overlapping Coins" configurations as experimentally observed [46].
For large platelets and high charge anisotropy, a phase separation between an equilibrium gel and a isotropic liquid phase is predicted at low volume fractions. The threshold volume fraction value at which the phase separation occurs is further found to increase with salt concentration. The same observations made for aged laponite dispersions, although the phase separated samples were found at lower volume fractions [46,47].
At intermediate charge anisotropy, a gel forms from a sol of clusters of individual particles randomly oriented that progressively grows with volume fraction in qualitative agreement with observations in montmorillonite clay dispersed in low pH and salt concentration aqueous solutions.
For entirely negatively charged platelets, a transition from an isotropic liquid to a glass phase occurs. This transition is favored for small particles in agreement with experimental observations on natural clay dispersions at neutral pH [48]. Reversely, the sol-gel transition and liquid-gel separation are found to be favored for large particles bearing a weak and strong charge anisotropy, respectively.
Finally, in the case of strong charge anisotropy, the liquid-gel separation is predicted to disappear in favor of a sol-gel transition upon decreasing the size of platelets. This is depicted by papers II and III.

7.3 Liquid crystal formation

Several liquid crystal phases were encountered throughout the studies. Their formation is studied as a function of charge anisotropy, ionic strength and size of the platelets in papers II-IV.

- A smectic B phase is found for volume fractions between 1 and 7% and low salt concentration ($<$ 10mM). Its formation is only observed when the particles bear a strong charge anisotropy. This phase dissolves at high salt concentration. Note that, it is the first time that such a phase is predicted for charged plate-like particles dispersed in an aqueous solvent.

[46] P. Mongondry, J. F. Tassin, and T. Nicolai, J. Coll. Interface Sci. **283**, 397 (2005).
[47] B. Ruzicka, E. Zacarelli, L. Zulian, R. Angelini, M. Sztucki, A. Moussaid, T. Narayanan, and F. Sciortino, Nature Mat. **10**, 50 (2011).
[48] L. J. Michot, C. Baravian, I. Bihannic, S. Maddi, C. Moyne, J. F. L. Duval, P. Levitz, and P. Davidson, Langmuir **25**, 125 (2009).

- The formation of the nematic phase has been shown to be favored by low aspect ratio for neutral platelets [16]. This result is also found in our simulations. Its formation is predicted to be further favored for uniformly charged platelets. Reversely, the presence of a charge anisotropy, i.e. positive charges on the edges, hinders the formation of a nematic phase. The latest is shown to disappear when the charge anisotropy is too strong. The isotropic-nematic transition is often close or pre-empted by a liquid-solid transition. We found that a true liquid-nematic transition may occurs when the platelets carry a low charge anisotropy or are entirely negatively charged.
- Finally, columnar phases are encountered for high volume fractions. Their formation is found to be favored by high charge anisotropy and low ionic strength. Depending on the positive charge distribution on the edges and the salt concentration, new columnar phases were discovered as *the zig-zag columnar phase, the interpenetrated rectangular and hexagonal columnar phases*. The latter was also recently predicted by Morales-Andra [49].

7.4 Growth and stability of nanoplatelets

In paper V, the growth of C-S-H nanoplatelets is shown to be limited by their own internal electrostatic repulsions. We also study in some details the stability of such particles in calcium salt solutions and discuss the possible consequences on the kinetic competition between the growth and aggregation of C-S-H platelets. Finally, we investigate the different modes of aggregation of these platelets onto C_3S grain surfaces. In agreement with experimental observations[50,51], it is found that a high calcium concentration and pH enhance the axial "growth" of the platelets, whereas opposite conditions enhance a lateral "growth".

7.5 Concluding remarks

In this book, I present the results I obtained when investigating several scientific problems by the use and development of computer simulations. The goal was not only to create theoretical models but also to bridge experiments and theories in order to give further insights into complicated physico-chemical

[49] L. Morales-Andra, H. H. Wensink, A. Galindo, and A. Gil-Villegas, J. Chem. Phys. **136**, 034901 (2012).
[50] S. Garrault and A. Nonat, Langmuir **17**, 8131 (2001).
[51] S. Garrault, E. Lesniewska, and A. Nonat, Material and Structures **38**, 435 (2005).

systems. The whole range of systems and chemical phenomena considered clearly demonstrate the importance of the study of plate-like particles, more especially as these results are relevant to many other systems.

The development of a model able to reproduce the main behavior and the complete phase diagram of charged plate-like particle suspensions has been an ongoing project for 30 years in physical chemistry. This thesis is a new step in this direction. It shows that the underlying physics of clays and C-S-H in aqueous solution can be partially captured by the use of simple models and theories. Further investigations involving more sophisticated theories or different techniques are of course needed to complete the picture.

An interesting aspect with computational physical chemistry is that computer power increases rapidly with time. There is no doubt that, in few years time, one will be able to approach scientific problems with a much more detailed description of the systems. This is a good thing considering the number of unanswered questions related to the behavior of dispersions of mineral plate-like particles.

Finally, I hope that the reader has found some interest in the work presented in this book and that the results will inspire further experimental and theoretical investigations.

Acknowledgements

I would like first to thank **Christophe** and **Bo** for giving me the opportunity to live this adventure in Sweden, for ALL support, explanations, scientific and personal discussions, encouraging words and interesting projects all along those four and a half years. Thank you for helping me to cross the line from student to researcher, even if it has not always been easy. For sure you have shaped who I am today and I am more than grateful for that. Thanks also to **André** for his advices in the different projects and his jokes in the coffee room.

Thanks to all seniors in France and Sweden and more particularly: **Mikael** for all your help and support and for being an attentive ear to me, **Magnus** for your scientific expertise and for sharing interest in music and drawings, **Jan** for all tips, **Marie** for all interesting seminars, and **Torbjörn** for always taking the time to answer my questions and for all clear explanations.

Martin Trulle, my swedish brother, thank you for making me discover how fun Sweden can be. Thanks also for ALL your help and interesting discussions (scientific or not) during those years.
Martin Ture and **Fabrice**, thanks to both of you for the nice discussions, strong support and all the laughs during the Cappucino and Mac Carthy's evenings.
Marie-Céline and **Mickael**, thanks for all the french evening shared in Sweden and for the moral support!
Björn, thank you for being a good course companion and for the help you provided me.
Segad, for being my office-mate and for the nice discussions.
Anil, for your joy and being the guardian for my bike.
Gleb, thank you for being a good "camping" buddy.
Sofi, thanks a lot for the strong support in the last weeks before printing the thesis.

I also want to thanks all other phD or postdoc that crossed my way during these years. In Sweden: **Jimmy**, **Pär**, **Jonas**, **Asbjörn**, **Samuel**, **Svante**, **Paulius**, **Ryan**, **Marta**, **Axel**, **Fei**, **Joao**, **Olof** in theoretical chemistry, **John**, **Jenny**, **Joakim**, **Nina**, **Luis**, **Salome**, **Agnieszka**, **Sanna**, **Charlotte**, **Patrick**,

Marianna in physical chemistry, and **Stina**, **Johan** and **Eric** in biophysics. In France: **Fafa**, **Stephanie**, **Gilles**, **Jeremy**, **Florent**, **Semra**, **Fousia** and **Guillaume**.

A BIG thank you to all secretaries **Eva**, **Bodil** and **Ingrid** in Sweden and **Agnes** in France for all the help with the paper work. You really made my life a hundred time easier!

Thank you **Paula** for your infinite patience and for all the help with the printing of the thesis.

There is also a couple of friends I would like to thank for being around, for all the joy, fun, laugh and support they brought me. The gang of four: **Laurent**, **Guillaume**, and **Benoit**, you guys are the best buddies ever. Thanks also to those people for being part of my life for so long: **Fanny**, **David**, **Fabo**, **Mathias**, **Mika**, **Fran**, **Lovisa**, **Martin J** and **Daniel J**. Thanks also to **Manu**, **Bertrand**, **Steph** and **Jack Daniel** for all touring with the band. That was hell lot of fun. A stort tack till **Åsa** och **Håkan** for their kindness, all dinner invitations and winter bbq. Merci à ces personnes : **Marie-M**, **Sophie**, **Marjorie**, **Charlotte**, **Alrick**, **Alice F.**, **Pauline**, **Tristen**, **Sam**, **Alice C.**, **JB**, **Frank**, **Terese**, **Coralie** and **Paulina** pour avoir joué un rôle dans ma vie au cours de ces dernières années.

Enfin, je voudrais remercier les membres de ma famille pour leur indéfectible présence à mes côtés, leur soutien en toutes circonstances, leurs conseils avisés et leur amour. Un grand merci à **Papa**, **Maman**, **JB**, **Ludo**, **Alexia**, **Fanny**, **Laeti**, **Fred**, **Tata Joc.**, **Mamie** et **Robert**. Je voudrais finir ce livre en ayant une pensée pour mon grand père **Jean** et ma marraine **Françoise** qui ne me verront malheureusement jamais docteur.